Pressure-induced bcc to hcp transition in Fe: Magnetism-driven structure transformation

S. Mankovsky,[1] S. Polesya,[1] H. Ebert,[1] W. Bensch,[2] O. Mathon,[3] S. Pascarelli,[3] and J. Minár[1]
[1]*Fakultät Chemie/Physikalische Chemie, Universität München, Butenandtstr. 5-13, D-81377 München, Germany*
[2]*Institut für Anorganische Chemie, Christian-Albrechts-Universität zu Kiel, Max-Eyth-Str. 2, D-24118 Kiel, Germany*
[3]*European Synchrotron Radiation Facility, 6 Rue Horowitz 38043 Grenoble, France*
(Received 19 September 2013; published 25 November 2013)

The pressure induced bcc to hcp transition in Fe has been investigated via *ab initio* electronic structure calculations. It is found by the disordered local moment (DLM) calculations that the temperature induced spin fluctuations result in the decrease of the energy of Burgers type lattice distortions and softening of the transverse N-point TA_1 phonon mode with $[\bar{1}10]$ polarization. As a consequence, spin disorder in an system leads to the increase of the amplitude of atomic displacements. On the other hand, the exchange coupling parameters obtained in our calculations strongly decrease at large amplitude of lattice distortions. This results in a mutual interrelation of structural and magnetic degrees of freedom leading to the instability of the bcc structure under pressure at finite temperature.

DOI: 10.1103/PhysRevB.88.184108 PACS number(s): 75.50.Bb, 81.30.Hd, 71.20.Be, 78.70.Dm

I. INTRODUCTION

Since many years, considerable effort has been made to investigate the problem of nucleation and growth of a new phase upon martensitic transformation. Despite these attempts, there is no clear understanding so far of the atomic scale mechanism of the bcc-hcp reconstructive transformation occurring even in nonmagnetic materials. In the case of Fe—considered here—there are convincing arguments, both from theoretical and experimental sides, that magnetism plays a crucial role for the stability of bcc structure, making the problem more complicated.[1–6]

The bcc-hcp transformation observed in nonmagnetic materials has been extensively discussed in the literature.[7–12] The corresponding mechanism suggested by Burgers[13] consists in two types of simultaneous distortions (see Appendix, Fig. 9): (i) opposite displacement of adjacent (110) planes along the $[110]_{\mathrm{bcc}}$ direction, described by the parameter δ, associated with the transverse N-point TA_1 phonon mode with $[\bar{1}10]$ polarization; (ii) shear deformation along the [001] direction, characterized by the angle θ between the diagonals in (110) plane, which should change from 109.5° in the case of bcc structure to 120° in the case of hcp structure. The shear modulus is determined by the slope of the TA_1 phonon branch $[\xi,\xi,2\xi]$ with $[11\bar{1}]$ polarization.

Note that even for nonmagnetic materials a phenomenological description of this type of martensitic transformation is not straightforward: as pointed out in the literature,[7–12] the transition is discontinuous, having large critical displacements and no group-subgroup relationship between the symmetries of the initial and final phases. This causes problems for a Landau free energy expansion with respect to an order parameter. To deal with first-order transitions, the phenomenological Landau theory was extended[7,8,14] using two order parameters representing shuffle and shear deformations and have been applied rather successfully to the bcc-hcp phase transitions in Ti[15] and Zr,[16] associated with the softening of the N point TA_1 phonon mode. According to these theoretical findings, already small phonon softening (as it takes place in the case of Ti and Zr) can be sufficient for a first order transformation.[4,14–16]

The theoretical approach used for nonmagnetic systems has been applied to Fe, showing the important role of magnetism. In contrast to the nonmagnetic bcc metals mentioned above, no softening of the N point phonon modes have been observed under pressure neither experimentally up to 10 GPa[17–19] nor theoretically.[3,20] However, some DFT based theoretical investigations report about the key role of the shear stress in Fe under pressure for the bcc-hcp transition.[21,22] Their role has been investigated by Sanati *et al.*[14] in application to Ti and Zr showing that the bcc structure in these materials is completely stable with respect to shear deformation and only the N point phonon mode is responsible for bcc-hcp transformation.

Ab initio investigations by Ekman *et al.*[3] clearly showed that the stability of the bcc phase of Fe is due to magnetic ordering. They have shown that the Burgers type of lattice distortion results in the transition to the paramagnetic state at a certain amplitude of the atomic displacements and that way to the instability of the bcc structure. Liu and Johnson[4] have analyzed the potential-energy surface and minimum-energy pathway obtained within *ab initio* calculations and have also found that the magnetization collapse during the shuffle-shear (Burgers type) deformation leads to the instability of the bcc phase of Fe under pressure. A new mechanism for the bcc-hcp transition was suggested recently by Dupé *et al.*[23] pointing out that the shuffle and shear deformations in bcc Fe have different time scales that allows their independent treatment. The authors stress also that the new mechanism requires some peculiar magnetic order for the distorted state, which is different from the magnetic order of bcc and hcp phases.

To investigate experimentally the role of magnetism in the bcc-hcp transformation, Mathon *et al.*[2] have performed measurements of near edge x-ray absorption (XANES) including a determination of the x-ray magnetic circular dichroism (XMCD) for Fe under pressure. The high sensitivity of XMCD allows very precise measurements of the ordered magnetic moment on the absorber at the magnetic phase transition and to observe its correlation with the local geometrical structure monitored via XANES. The pressure dependence of the XMCD and XANES spectra around the transition pressure

 ©2013 American Physical Society

suggests that the magnetic transition slightly precedes the structural one. This finding allowed the authors to ascribe a leading role in the bcc-hcp transformation to the magnetic order in the system. Nevertheless, this interrelation requires further clarification, because, in general, the vanishing of magnetism should lead immediately to the instability of the bcc state and therefore, no difference in the transition pressure deduced from XANES and XMCD spectra should be expected.

Although these results give information on the origin of the pressure induced instability of bcc Fe and showing the minimal-energy pathway for the transition, there is still the question how the instability condition, which needs a certain phonon softening under pressure occurs while no softening could be found. One possible way has been suggested by Vul and Harmon[24] in their fluctuationless mechanism for martensitic transformations triggered by the defects presented in the crystal. In the present work, we analyze the conditions that can result in the instability in perfect bcc Fe via lattice fluctuations, in particular, the effect of temperature induced spin fluctuations for the bcc-hcp transition. These investigations in particular give an answer to the question, why the decrease of the XMCD signal slightly precedes that of the XANES signal corresponding to bcc structure upon a pressure increase.

II. THEORETICAL INVESTIGATIONS

A. Details of calculations

Spin-polarized electronic structure calculations have been performed using the spin-polarized KKR (Korringa-Kohn-Rostoker) Green's function method[25] in the fully relativistic approach. The generalized gradient approximation (GGA) for density functional theory was used with the exchange-correlation potential due to Perdew, Burke, Ernzerhof (PBE).[26] The potential was treated within the full potential (FP) scheme. For the angular momentum expansion of the Green's function, a cutoff of $l_{\max} = 4$ was applied. To treat spin disorder in the system, the self-consistent coherent potential approximation (CPA) method was employed. For the calculation of the x-ray absorption coefficient $\mu^{\vec{q}\lambda}$, the following expression has been used:

$$\mu^{\vec{q}\lambda}(\omega) \propto \sum_{i\,\mathrm{occ}} \langle \Psi_i \hat{X}_{\vec{q}\lambda} \Im G^{+}(E_i+\omega)\, \hat{X}^{\times}_{\vec{q}\lambda} \Psi_i \rangle\, \Theta(E_i+\omega-E_F), \tag{1}$$

where $\vec{q}$, ω, and λ stand for the wave vector, frequency, and polarization of the radiation, and $\hat{X}_{\vec{q}\lambda}$ is the electron-photon interaction operator.[27]

The finite temperature magnetic properties have been investigated via Monte Carlo (MC) simulations based on the classical Heisenberg model, using a standard Metropolis algorithm.[28] The exchange coupling parameters J_{ij} for these calculations are obtained within the approach described by Lichtenstein.[29,30]

B. Total energy calculations for the bcc-structure

Figure 1 represents the results of total energy calculations for bcc Fe in ferromagnetic (FM) and nonmagnetic (NM) states as well as for hcp structure in the NM state. (Below, we will use the notation NM and PM to denote the nonmagnetic state with with zero magnetic moments and the paramagnetic state implying a random distribution of the localized magnetic moments, respectively.) The calculations for the hcp structure have been performed at a fixed c/a ratio equal to 1.596. According to the results shown in Fig. 1, the minimum of the total energy corresponds to the equilibrium lattice parameter $a = 5.37$ a.u. in the case of the FM state of bcc-Fe, and in the case of hcp-Fe, to $a = 4.66$ a.u. The critical pressure evaluated from the equivalence of the enthalpy of the bcc and hcp phases is equal to 8 GPa in reasonable agreement with experiment.

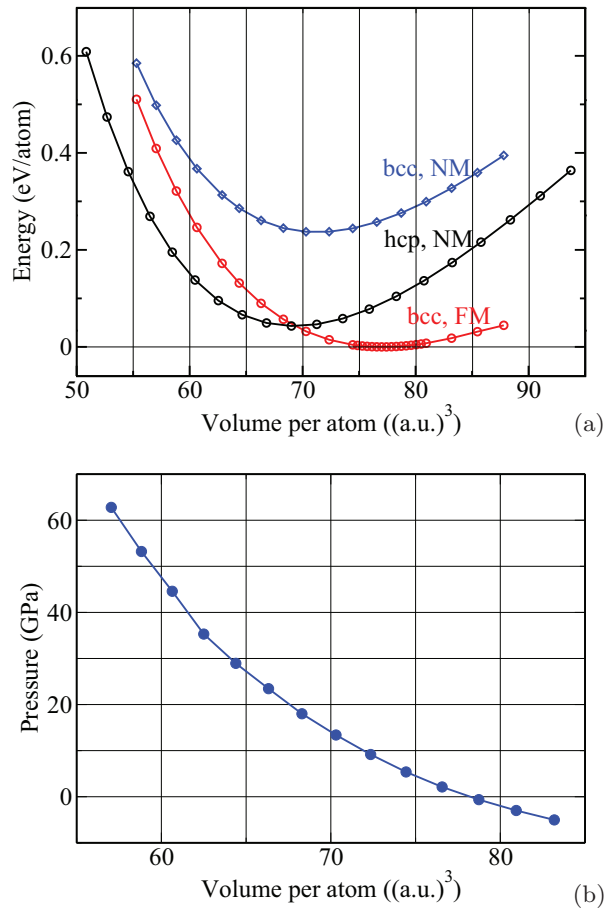

FIG. 1. (Color online) (a) Total energy as a function of volume for ferromagnetic (FM) and nonmagnetic (NM) states of bcc-Fe as well as for NM state of hcp-Fe. (b) Pressure as a function of volume for bcc-Fe.

The FM to NM transition leading to the instability of the bcc structure occurs at the lattice parameter $a \approx 4.6$ a.u. [$V \approx 48.7$ (a.u.)^3, Fig. 1] that corresponds to a pressure of about 200 GPa. This value is much too high when compared directly to experiment. Therefore this type of instability does not seem to play a role for the real system.

C. Total energy calculations for the distorted bcc Fe

The energy of Burgers type lattice distortion in bcc Fe have been calculated first assuming FM order in the system. In contrast to the works of Ekman[3] and Vul and Harmon,[24] where the authors used two parameters θ and δ to describe the shear deformation within the (110) plane and displacements

of the neighbor (110) planes with respect to each other (see Introduction), in the present investigations we consider the path from bcc to hcp transformation as suggested by Friak and Sob,[31] which includes both deformations using only one parameter Δ (see Appendix). This approach avoids the high-energy configurations occurring upon independent variation of the parameters δ and θ, accounting only those being close to the minimum total energy path.[31] The parameter $\Delta = 0$ corresponds to the bcc structure, while $\Delta = 1$ corresponds to the hcp structure with $c/a = \sqrt{8/3}$. As soon as additional calculations (not presented here) exhibit only a weak dependence on the c/a ratio for the position of the minimum of total energy as a function of lattice parameter, the following discussion concerns the results for $c/a = \sqrt{8/3}$ for the sake of convenience.

Figure 2 represents the total energy as a function of the parameter Δ, $E(\Delta)$, for different lattice parameters a corresponding to different pressure values. The $E(\Delta)$ curves have two minima corresponding to the FM bcc structure ($\Delta = 0$) and NM hcp structure ($\Delta = 1$), which is a quasi-equilibrium state. At low pressure, the FM bcc structure of Fe is more stable, while as pressure increases, the energy of the NM hcp structure becomes deeper leading to the stability of this state. Note that the $E(\Delta)$ curves (see Fig. 2) calculated for three different pressure values (or, equivalently, lattice parameters a equal to 5.1, 5.2, and 5.3 a.u.) for the FM state of Fe, have nearly the same dispersion. This is in line with previous phonon calculations exhibiting no softening of the N-point phonon modes under pressure as discussed above.

As follows from Fig. 1, the NM state of bcc Fe is higher in energy than the FM state. $E_{\rm FM}(\Delta)$ increases while $E_{\rm NM}(\Delta)$ decreases monotonously with Δ varying from 0 to 1 (open symbols in Fig. 2), indicating the instability of NM bcc Fe with respect to this type of distortions, in line with the results on phonon calculations.[3,20] The "critical" distortion values, Δ_c, correspond to the cross-points of the total energy curves as functions of the lattice distortion Δ, calculated for the FM $[E_{\rm FM}(\Delta)]$ and NM $[E_{\rm NM}(\Delta)]$ states. That is, at the critical values of distortions, $E_{\rm FM}(\Delta_c) = E_{\rm NM}(\Delta_c)$. The magnitude of the energy cusps in Fig. 2, defined by $E_{\rm ci} = E_{\rm NM} = E_{\rm FM}$

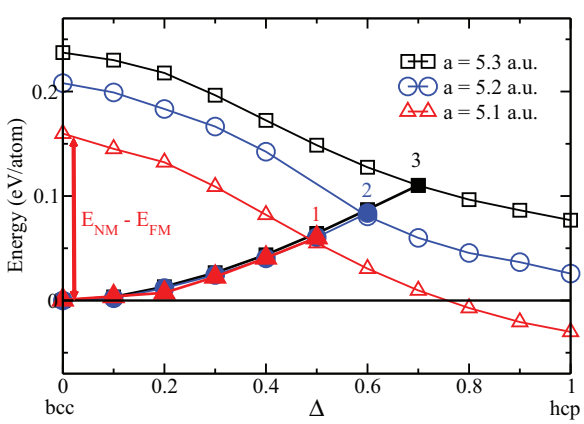

FIG. 2. (Color online) Energy as a function of the parameter Δ. Full symbols correspond to the FM state, open symbols to the NM state. The vertical arrow indicates the energy difference $\Delta E = E_{\rm NM} - E_{\rm FM}$.

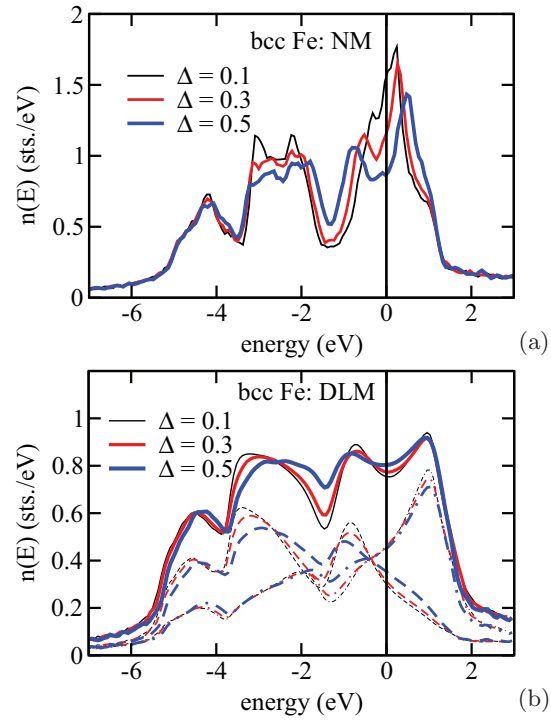

FIG. 3. (Color online) Total DOS per atom as a functions of the parameter Δ for Pauli paramagnetic (nonmagnetic) (a) and paramagnetic (via DLM calculations) (b) states of bcc Fe. Dashed (dashed-dotted) lines represent spin-up (spin-down) states.

for the various lattice parameters a_i, E_{c1}, E_{c2}, E_{c3} and corresponding amplitude of the "critical" distortions (Δ_{c1}, Δ_{c2}, and Δ_{c3}) are getting smaller when the pressure increases.

Figure 3(a) shows the DOS, $n(E)$, corresponding to the NM state of distorted bcc Fe. For small distortions, $n(E)$ has a maximum at the Fermi level E_F indicating the instability of the NM state. This DOS maximum is formed by the double-degenerated e_g electronic energy bands. Therefore there are two scenarios to remove the instability by breaking the symmetry of the system: either due to structure distortion (e.g., Burgers distortion) leading to the splitting of doubly degenerated e_g states at E_F or due to spontaneous magnetization leading to the exchange splitting of the electronic states having opposite spin directions. At ambient pressure the second scenario is more favorable leading to the stabilization of the bcc structure with FM order. Under high pressure, however, due to a reduced tendency towards spontaneous magnetization via the Stoner mechanism the first scenario (structure distortion) could be more preferable, as discussed by Ekman.[3] The same effect can be achieved even at lower pressure, when the amplitude of the distortion is big enough, as demonstrated in Fig. 2 by the "critical" points 1,2, and 3. However, in this case, the energy barrier $E_{\rm FM}(\Delta_c) - E_{\rm FM}(\Delta = 0)$ is much too high to be overcome assuming the fluctuation mechanism of phase transition, even at the pressure $p \approx 23$ GPa ($a = 5.1$ a.u.), when the hcp structure becomes energetically more preferable.

So far, we have discussed the stability of the system with respect to lattice distortions assuming no deviations from perfect FM order. To discuss in more details the interrelation between the structural and magnetic degrees of freedom, the

effect of spin moment fluctuations should also be investigated. Moreover, such investigations are required to account for the conditions of the experimental measurements performed at room temperature. To take the effect of temperature induced spin fluctuations at $T > T_c$ into account, the paramagnetic state with nonzero local moments of Fe was simulated using the so-called disordered local moment (DLM) scheme describing a random distribution of the local magnetic moments over the lattice sites. Accordingly, discussing the results of calculations for the PM state we will use the term "DLM state" implying the approximation used in these calculations. The DLM calculations are done by means of the CPA alloy theory applied to the effective alloy, $Fe_x^+Fe_{1-x}^-$, with equal amount of "alloy" component ($x = 0.5$) having the spin magnetic moment along the $+z$ direction (Fe^+) and in the opposite direction (Fe^-).[32,33] The expression for the exchange coupling parameters[29,30] in this case has been modified to deal with the effective CPA medium (representing the random crystal potential) described by the effective scattering path operator. As a result, it uses the element-projected scattering path operators associated with the atoms having "up" and "down" magnetic moment directions (Fe^+ and Fe^-), as it was discussed, e.g., in Ref. 34.

The E dependence on Δ for the PM state obtained (via DLM) at the pressure corresponding to $a = 5.2$ a.u. is shown in Fig. 4(a) by solid circles. For $\Delta = 0$ (i.e. ideal bcc structure), the difference $E_{PM}(\Delta = 0) - E_{FM}(\Delta = 0)$ is about two times smaller than $E_{NM}(\Delta = 0) - E_{FM}(\Delta = 0)$. $E_{PM}(\Delta)$ decreases slowly with Δ varying from 0 to 1, indicating an instability of the DLM state of bcc Fe at this pressure value. Note that the $E(\Delta)$ dependence for DLM state, $E_{PM}(\Delta)$, is weaker than that corresponding to the NM state, $E_{NM}(\Delta)$. This behavior can be understood using the DOS plots shown in Fig. 3. In the case of DLM state, one can clearly see a local DOS minimum [see Fig. 3(b)] at the Fermi energy, created by the exchange-split majority and minority d-states of Fe. The dependence on Δ of the DOS obtained for DLM state is rather weak, in contrast to the DOS obtained for the NM state [see Fig. 3(a)], having a pronounced maximum at E_F strongly modified due to Burgers type of distortions.

However, instability of the DLM state of bcc Fe with respect to the lattice distortion Δ occurs only at the pressure exceeding a certain critical value [closed circles and squares in Fig. 4(b)]. In the vicinity of ambient pressure, the $E_{PM}(\Delta)$ curve has a minimum at $\Delta = 0$ [closed triangles in Fig. 4(b)], that means stability of this state with respect to Burgers distortions.

To simulate the magnetic disorder corresponding to the temperature below the critical one, T_C, so-called noncompensated DLM (NDLM) calculations have been performed with the NDLM state simulated by an effective alloy $Fe_{1-x}^+Fe_x^-$ with $x \in [0.0,0.5]$. In this case, the normalized magnetic moment $M/M_s = (M_s n_+ - M_s n_-)/M_s$ at each lattice site is equal to $(1 - 2x)$, assuming M_s to be a saturated local spin magnetic moment of the Fe atoms. Open circles in Fig. 4(a) correspond to the NDLM state of bcc Fe ($a = 5.2$ a.u.) with $M/M_s = 0.5$. In this case, the curve $E(\Delta)$ has a minimum at $\Delta = 0$ [open circles in Fig. 4(b)] and exhibits a slow increase with Δ increasing up to the critical displacement $\Delta_c \approx 0.25$. The total energy $E_{NDLM}(\Delta = 0)$ decreases further, when M/M_s changes up to $M/M_s = 1$, which is associated with the temperature decrease and increase of FM order. As an example, open

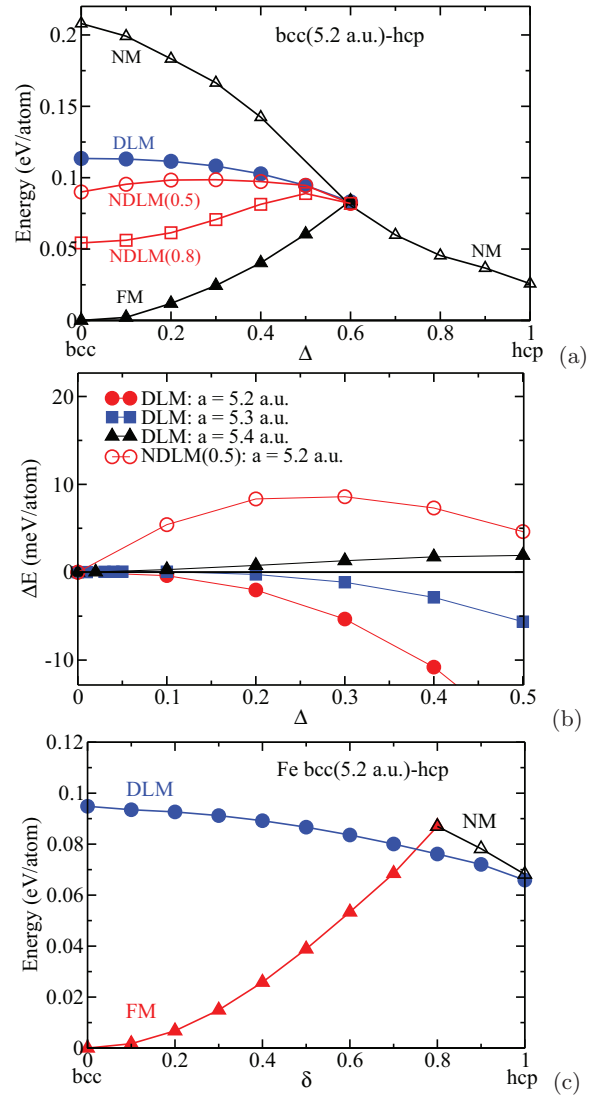

FIG. 4. (Color online) Total energy as a function of the lattice distortion parameter Δ for bcc Fe with $a = 5.2$ a.u.: (a) comparison of the results for FM (triangles), PM (DLM, closed circles), partially disordered FM (NDLM) with noncompensated magnetic moment $M/M_s = 0.5$ (opened circles), and $M/M_s = 0.8$ (opened squares); (b) comparison of the DLM and NDLM ($M/M_s = 0.5$) results for different lattice parameters; (c) total energy as a function of the amplitude of the N point TA_1 phonon mode for FM state (closed triangles), NM state (opened triangles), and DLM state (closed circles).

squares in Fig. 4(a) represent the $E_{NDLM}(\Delta)$ dependence for $M/M_s = 0.8$ (i.e., $x = 0.1$). Thus the energy of Burgers type lattice distortions, $E(\Delta) - E(0)$, decreases in the presence of temperature induced magnetic disorder and close to the PM state (DLM state) becomes much smaller than in the case of perfect FM order. As a consequence, this leads to an increase of atomic displacements, caused directly by magnetic disorder in the system.

Additional calculations have been performed to check explicitly the influence of magnetic disorder on the energy of the N point TA_1 phonon mode (opposite displacement of adjacent (110) planes along the $[110]_{bcc}$ direction), i.e.,

without accounting for shear deformation along the [001] direction present in the case of the Burgers type deformation. The results are shown in Fig. 4(c). The energy dependence $E(\delta)$ on the atomic displacements δ is rather similar to that obtained for the Burgers deformations, shown in Fig. 4(a). Thus these results show an explicit evidence of the crucial role of magnetic disorder for the softening of the N point TA_1 phonon mode making it responsible as the driving mechanism for the bcc to hcp transition.

Additional investigations have been performed to show an effect of lattice displacements on the magnetic order in the system. Considering atomic fluctuations corresponding to the Burgers type of lattice deformation,[31] two series of the exchange coupling parameters, J_{ij}, have been calculated for the DLM state: (1) for different pressure values (i.e., different lattice parameters) for the perfect bcc structure and (2) for the distorted bcc lattice with $a = 5.2$ a.u. with different distortion parameter Δ. Figure 5 shows the results for the case 1, for which J_{ij} values are presented together with corresponding Curie temperatures, determined by means of MC simulation, and exhibiting their decrease when the pressure increases. These results are in good agreement with theoretical results obtained by other authors within the DLM scheme[34,35] despite some differences related to the details of the calculations. In particular, the differences can be ascribed to the different type of exchange-correlation potential (as shown by Ruban[35]), to different approximations used for the atomic potential [e.g., ASA (atomic sphere approximation) versus FP used in the present work], and so on. The exchange coupling parameters J_{ij} for distorted bcc Fe (case 2) are shown in Fig. 6 where one can easily see that lattice Burgers distortions are accompanied by pronounced variations of the exchange coupling parameters. In particular, we can point out a decrease of the FM and increase of the AFM exchange interactions when the Δ parameter increases.

Assuming that the biggest amplitude of atomic displacements is related to this type of distortions (due to their softening), the corresponding critical temperature have been calculated using the simulations for different values for the

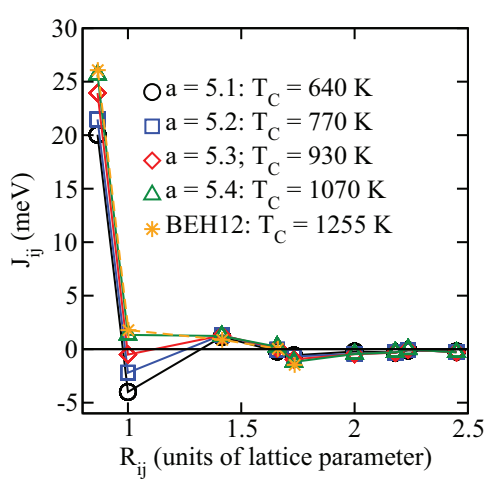

FIG. 5. (Color online) (a) Exchange coupling parameters for bcc Fe at different lattice parameter via DLM calculations for case 1 (see text). For comparison, the results for J_{ij}^{eff} obtained by Böttcher *et al.*[34] ($c_{\mathrm{Fe}^+} = c_{\mathrm{Fe}^-} = 0.5$) are presented pointed by asterisks.

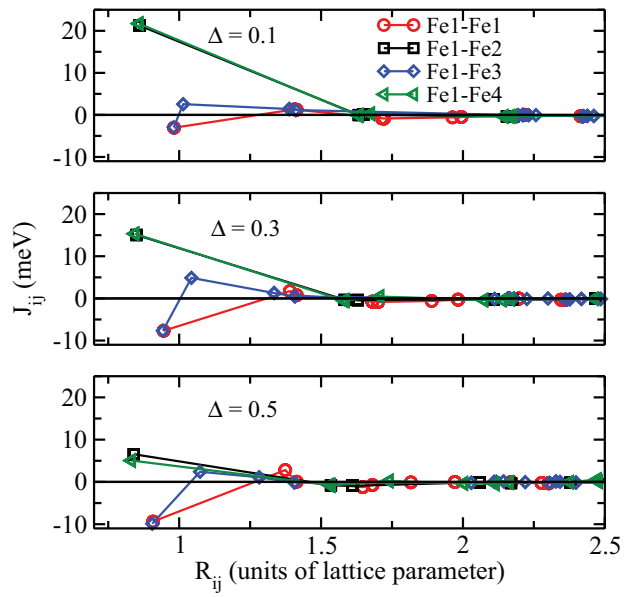

FIG. 6. (Color online) Dependence of the exchange coupling parameters on the amplitude of lattice distortion for bcc Fe under pressure corresponding to lattice parameter $a = 5.2$ a.u. for case 2 (see text).

Δ parameter [see Fig. 7(a)]. This simplified approach was used to demonstrate the effect of atomic displacements on the finite-temperature magnetic properties of Fe under fixed pressure (corresponding to $a = 5.2$ a.u.). At small distortions, the system has FM order with the Curie temperature decreasing upon Δ increase. At $\Delta \geqslant 0.3$, the system exhibits AFM properties (noncollinear or collinear, depending on Δ). The

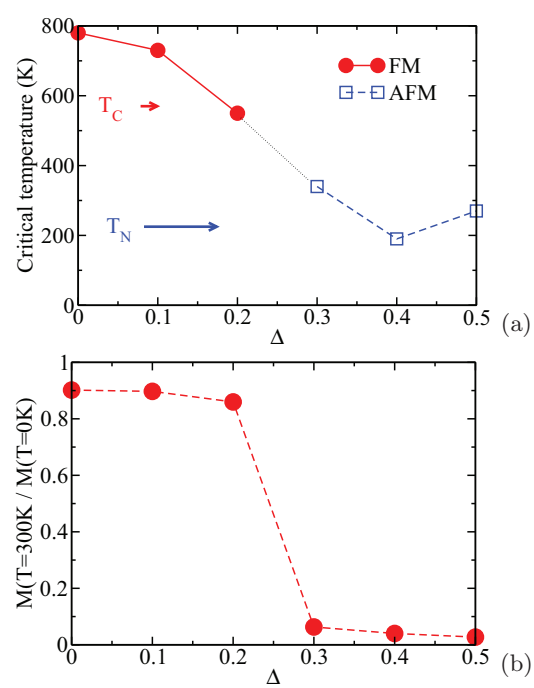

FIG. 7. (Color online) Results of MC simulations: (a) critical temperature as a function of lattice distortion Δ for bcc Fe with $a = 5.2$ a.u. and (b) the normalized average magnetic moment corresponding to the temperature $T = 300$ K.

average magnetic moment calculated for different Δ values at the temperature $T = 300$ K is presented in Fig. 7(b). It drops down at rather small lattice distortions, $\Delta > 0.2$, first, due to transition to the state with noncollinear magnetic structure and then, for $\Delta > 0.3$, to the PM state.

In spite the simplifications used for our analysis, the results presented above directly demonstrate the strong mutual influence of the lattice Burgers distortion and spin moment fluctuations resulting in a pronounced pressure and temperature dependence of the geometric and magnetic structure in the system. Both effects are the counterparts of the mechanism leading to a softening of the corresponding phonon modes responsible for the instability of the bcc state of Fe and leading to the bcc-hcp transition.

D. Experimental observations versus theory: *K*-edge XMCD

Experimental investigations on bcc Fe under pressure have been performed using x-ray absorption spectroscopy at the K edge of Fe, with the XANES and XMCD spectra measured simultaneously.[2] This allowed to check experimentally the role of magnetic order for the stability of bcc-Fe, as discussed in the literature (see, e.g., Ref. 3). In particular, a synchronous decrease of the "structural" and "magnetic" XAS signals related to the ferromagnetic bcc phase of Fe would be expected at the critical pressure, where this loss of stability is associated with a transition to the Pauli paramagnetic (i.e., NM) state.

Theoretical calculations of the x-ray absorption and XMCD spectra at the K edge of Fe have been performed for different lattice parameters corresponding to the pressure values below the critical one. These results are compared in Fig. 8 with experimental spectra measured at different pressures below the critical value. In this case, the spectra are associated to the bcc structure with a slow variation upon pressure increase caused by the pressure induced variation of the lattice parameter. As one can see, the theoretical calculations reproduce the experimental XANES results quite well. The same applies for the XMCD spectra. At the pressure above the critical value, the XANES spectrum reflects the hcp structure and is again in good agreement with experiment (see Fig. 8). In this case the pronounced peaks at ≈90 and 110 eV, specific for the bcc structure have disappeared, while new ones characterizing the hcp phase occur at the energy ≈50 eV and just above 100 eV. The XMCD signal above the critical pressure is very weak and corresponds to the remnant bcc phase at this pressure, which disappears completely if the pressure is further increased.

To explain the pressure dependence of the experimental XMCD spectra, we refer to the theoretical results discussed above. The XANES experiment performed at the K edge of Fe implies that the induced orbital polarization of the p-electrons is probed. In ordered FM systems this implies that the K edge XMCD signal should be roughly proportional to the spin magnetic moment of the $3d$ electrons (see, e.g., Refs. 36,37 and references therein). At finite temperature, however, a decrease of the dichroic signal can occur due to an increase of the magnetic disorder in the system, even for weak changes of the local magnetic moment. In the present case of bcc Fe at fixed (room) temperature, the increase of the magnetic disorder is governed by the increasing pressure. At the same time, the XANES signal does not change because the bcc structure remains stable until the critical value of the magnetic disorder (associated with a critical pressure) is reached. This is indeed observed in the experimental XMCD spectra. A further pressure increase should result in a quick drop down for the average magnetic moment leading to the instability of the bcc structure and to a transition to the hcp phase, as it is observed in the XANES and XMCD spectra.

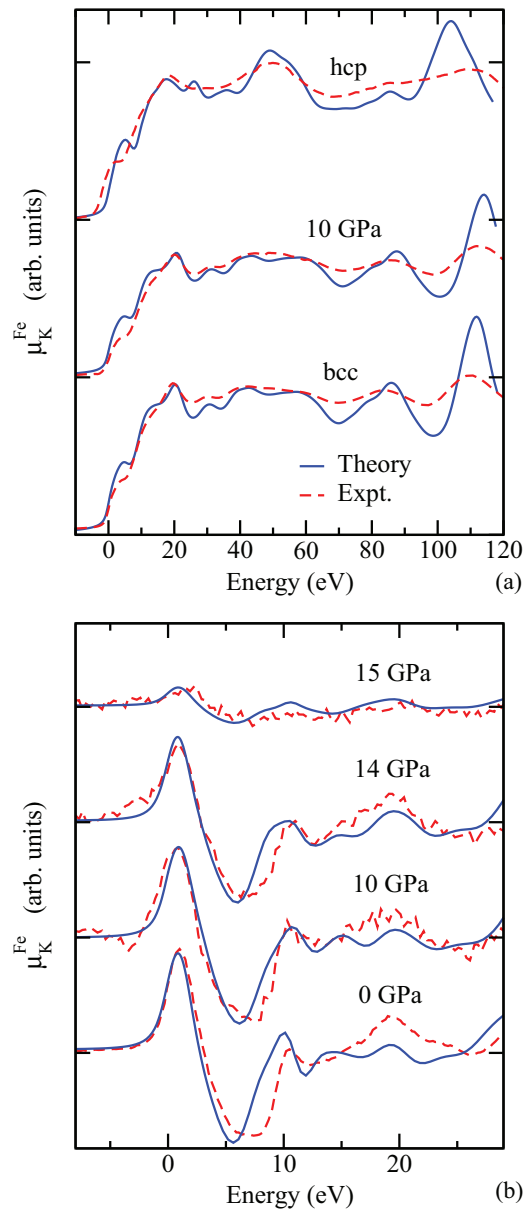

FIG. 8. (Color online) K-edge XANES for bcc Fe at different pressures as well as hcp Fe at a pressure above the critical one: (a) XANES and (b) XMCD spectra. Solid and dashed lines correspond to theoretical and experimental results, respectively.

III. SUMMARY

In summary, our investigations led to the following results: (i) assuming no structural nor spin distortions for bcc Fe, a transition to the hcp structure can occur only at very high pressures, corresponding to a lattice parameter ≈4.6 a.u., at which the system becomes paramagnetic; (ii) Burgers-type

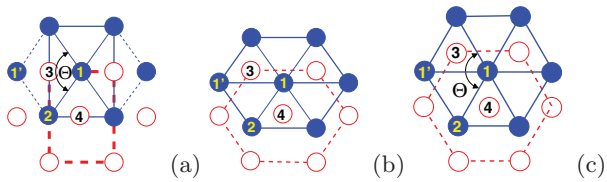

FIG. 9. (Color online) Transformation from bcc to hcp structure according to Burgers scheme: (a) (110) planes of the bcc structure; (b) opposite displacement of adjacent (110) planes along the $[110]_{bcc}$ direction; (c) hcp structure, after shear deformation along [001] direction with θ changing from 109.5^o in the case of bcc structure to 120°.

lattice distortions in collinear FM bcc Fe can lead to a transition to the NM state and as a result to the bcc-hcp transition at the pressure close to the one observed experimentally, implying fluctuation mechanism of transition. However, the energy of lattice fluctuations required for the FM-PM transition is too high; (iii) DLM calculations show an instability of spin disordered bcc Fe upon a pressure increase. This requires the transition to the PM state. To get this condition at the temperature of measurements, T_e, the Curie temperature should be low enough, i.e., $T_C < T_e$. However, this is not the case. On the other hand, even a partial spin disorder can result in the decrease of the energy of lattice fluctuations required for transition to the PM state. This implies that both effects, spin and lattice fluctuations, are the counterparts of the mechanism leading to a softening of the corresponding phonon modes responsible for the instability of the bcc state of Fe and leading to bcc-hcp transition.

ACKNOWLEDGMENTS

Financial support within the framework of Deutsches Elektronen-Synchrotron DESY (BMBF) 05K13WMA program, DFG FOR1346 program, and the priority Schwerpunktprogramm SPP1415 is gratefully acknowledged.

APPENDIX

According to Friak and Sob,[31] transformations using only one parameter Δ include both transformations represented by the parameters δ or θ (see Fig. 9), avoiding the high-energy configurations occurring upon their independent variation. Variation of Δ parameter keeping the volume $V(\Delta)$ unchanged leads to the hcp structure with the ratio $c/a = \sqrt{8/3}$, following the path being close to the minimum energy path.[31] The lattice parameters for the distorted orthorombic structure with 4 atoms/u.c. varies as follows:

$$a = a_0\sqrt{2}/(V/V_0)^{1/3},$$
$$b = a[\Delta(2\sqrt{3} - 3\sqrt{2})/6 + 2\sqrt{2}],$$
$$c = a[\Delta(2\sqrt{2} - 3)/3 + 1],$$
$$V/V_0 = \sqrt{2}[\Delta(2\sqrt{3} - 3\sqrt{2})/6 + 2\sqrt{2}][\Delta(2\sqrt{3} - 3)/3 + 1].$$

The atomic positions in the unit cell with distortion are (0,0,0),(1/2,1/2,0),(1/2 − Δ/6,0,1/2),(−Δ/6,1/2,1/2).

[1] J. P. Rueff, M. Krisch, Y. Q. Cai, A. Kaprolat, M. Hanfland, M. Lorenzen, C. Masciovecchio, R. Verbeni, and F. Sette, Phys. Rev. B **60**, 14510 (1999).
[2] O. Mathon, F. Baudelet, J. P. Itié, A. Polian, M. d'Astuto, J. C. Chervin, and S. Pascarelli, Phys. Rev. Lett. **93**, 255503 (2004).
[3] M. Ekman, B. Sadigh, K. Einarsdotter, and P. Blaha, Phys. Rev. B **58**, 5296 (1998).
[4] J. B. Liu and D. D. Johnson, Phys. Rev. B **79**, 134113 (2009).
[5] I. Leonov, A. I. Poteryaev, V. I. Anisimov, and D. Vollhardt, Phys. Rev. B **85**, 020401 (2012).
[6] A. V. Ruban and V. I. Razumovskiy, Phys. Rev. B **85**, 174407 (2012).
[7] P.-A. Lindgard and O. G. Mouritsen, Phys. Rev. Lett. **57**, 2458 (1986).
[8] P. Tolédano, Z. Kristallogr. **220**, 672 (2005).
[9] V. P. Dmitriev, Y. M. Gufan, and P. Tolédano, Phys. Rev. B **44**, 7248 (1991).
[10] V. Dmitriev and P. Toledano, Phase Transitions **49**, 57 (1994).
[11] Y. A. Izyumov, V. M. Laptve, and V. N. Syromyatnikov, Phase Transitions **49**, 1 (1994).
[12] Y. Chen, K. M. Ho, and B. N. Harmon, Phys. Rev. B **37**, 283 (1988).
[13] W. G. Burgers, Physica **1**, 561 (1934).
[14] M. Sanati, A. Saxena, T. Lookman, and R. C. Albers, Phys. Rev. B **63**, 224114 (2001).
[15] W. Petry, A. Heiming, J. Trampenau, M. Alba, C. Herzig, H. R. Schober, and G. Vogl, Phys. Rev. B **43**, 10933 (1991).
[16] A. Heiming, W. Petry, J. Trampenau, M. Alba, C. Herzig, H. R. Schober, and G. Vogl, Phys. Rev. B **43**, 10948 (1991).
[17] V. J. Minkiewicz, G. Shirane, and R. Nathans, Phys. Rev. **162**, 528 (1967).
[18] B. N. Brockhouse, H. E. Abou-Helal, and E. D. Hallman, Solid State Commun. **5**, 211 (1967).
[19] S. Klotz and M. Braden, Phys. Rev. Lett. **85**, 3209 (2000).
[20] H. C. Hsueh, J. Crain, G. Y. Guo, H. Y. Chen, C. C. Lee, K. P. Chang, and H. L. Shih, Phys. Rev. B **66**, 052420 (2002).
[21] J. Zhao, D. Maroudas, and F. Milstein, Phys. Rev. B **62**, 13799 (2000).
[22] K. J. Caspersen, A. Lew, M. Ortiz, and E. A. Carter, Phys. Rev. Lett. **93**, 115501 (2004).
[23] B. Dupé, B. Amadon, Y.-P. Pellegrini, and C. Denoual, Phys. Rev. B **87**, 024103 (2013).
[24] D. A. Vul and B. N. Harmon, Phys. Rev. B **48**, 6880 (1993).
[25] H. Ebert, D. Ködderitzsch, and J. Minár, Rep. Prog. Phys. **74**, 096501 (2011).
[26] J. P. Perdew, K. Burke, and M. Ernzerhof, Phys. Rev. Lett. **77**, 3865 (1996).
[27] H. Ebert, Rep. Prog. Phys. **59**, 1665 (1996).
[28] K. Binder, Rep. Prog. Phys. **60**, 487 (1997).
[29] A. I. Liechtenstein, M. I. Katsnelson, and V. A. Gubanov, J. Phys. F **14**, L125 (1984).
[30] A. I. Liechtenstein, M. I. Katsnelson, V. P. Antropov, and V. A. Gubanov, J. Magn. Magn. Mater. **67**, 65 (1987).

[31]M. Friák and M. Šob, Phys. Rev. B **77**, 174117 (2008).
[32]J. Staunton, B. L. Gyorffy, A. J. Pindor, G. M. Stocks, and H. Winter, J. Magn. Magn. Mater. **45**, 15 (1984).
[33]B. L. Gyorffy, A. J. Pindor, J. Staunton, G. M. Stocks, and H. Winter, J. Phys. F **15**, 1337 (1985).
[34]D. Bottcher, A. Ernst, and J. Henk, J. Magn. Magn. Mater. **324**, 610 (2012).
[35]A. Ruban, *Psi-k Conference 2010, September 12-16, Berlin, 2009* (invited talk).
[36]V. Iota, J.-H. P. Klepeis, C.-S. Yoo, J. Lang, D. Haskel, and G. Srajer, Appl. Phys. Lett. **90**, 042505 (2007).
[37]R. Torchio, Y. O. Kvashnin, S. Pascarelli, O. Mathon, C. Marini, L. Genovese, P. Bruno, G. Garbarino, A. Dewaele, F. Occelli, and P. Loubeyre, Phys. Rev. Lett. **107**, 237202 (2011).